The Combined Strengthening Effect of CFRP Wrapping and NSM CFRP Laminates on the Flexural Behavior of Post-Tensioning Concrete Girders Subjected to Partially Strand Damage

Abbas Jalil Daraj
Department of Civil Engineering
University of Baghdad
Baghdad, Iraq
abbas19asdi@gmail.com

Alaa H. Al-Zuhairi
Department of Civil Engineering
University of Baghdad
Baghdad, Iraq
alaalwn@coeng.uobaghdad.edu.iq

Received: 23 April 2022 | Revised: 11 May 2022 | Accepted: 15 May 2022

Abstract-The studies on unbonded post-tensioned concrete members strengthened with Carbon Fiber Reinforced Polymers (CFRPs) are limited and the effect of strengthening on the strain of unbonded pre-stressed steel is not well characterized. Estimating the flexural capacity of unbound post-tensioned members using the design methodology specified in the design guidelines for FRP strengthening techniques of bonded post-tensioned members does not provide a reliable evaluation. This study investigates the behavior of unbonded post-tensioned concrete members with partial strand damage (14.3% and 28.6% damage) and strengthened with CFRP laminates using a near-surface mounted technique with and without U-wrap anchorages. The experimental results showed that the use of CFRP laminates significantly affects strand strain, especially with the use of anchors. The CFRP reinforcement affected flexural strength, crack width, and midspan deflection. However, the flexural stiffness of strengthened members during the serviceability phases is critical as strand damage ratios increase. In comparison with the nondamaged girder, the NSM-CFRP laminates enhanced the flexural capacity by 11% and 7.7% corresponding to strand damage of 14.3% and 28.6% respectively. Additionally, semiempirical equations were proposed to predict the actual strain of unbonded strands whilst considering the effects of FRP laminates. The suggested equations are simple to apply and provide accurate predictions with little variance.

Keywords-NSM-CFRP laminates; post-tensioned concrete; strand damage; strengthening

I. INTRODUCTION

Most standard investigations on the repair and strengthening of prestressed concrete members utilizing CFRP materials have recently concentrated on Pre-tensioned Concrete (PC) members, especially deteriorated or damaged due to corrosion or collision from overheight vehicles [1-3]. According to experimental tests, the use of CFRP strengthening techniques enhanced the stiffness and flexural strength of PC members, and reduced crack spacing and crack width [4-7]. The FRP reinforcement design guidelines cover two types of techniques. The first kind is External Bonded (EB), which involves bonding CFRP sheets or laminates to the tension surface of the concrete member. The second is the near-surface mounted technique, which requires extending CFRP bars or laminates into concrete cover grooves and attaching them with epoxy [8, 9]. The above techniques have many advantages, the most notable of which is that they are light-weight and improve flexural capacity, the Near-Surface Mounted (NSM) technique is gaining popularity since it is less prone to weather fluctuations and has the potential to delay or prevent FRP debonding [10]. The ACI 440-R of FRP strengthening has extensively documented the strengthening of prestressed concrete members, including bonded post-tensioned and pre-tensioned members, but unfortunately, these guidelines did not cover unbonded concrete members on the one hand, and these guidelines for strengthening were limited to the externally bonded technique on the other [11]. Unlike bonded post-tensioned members, which use the same concepts of equilibrium and strain compatibility to determine the strains in each of the pre-stressing steel, concrete, and CFRP components, the challenge for unbonded post-tensioned members is determining the pre-stressing steel strain increase due to the loss of strain compatibility between the pre-stressing steel and the surrounding concrete. Nonetheless, several researchers were able to develop methodologies that allowed them to predict the strain increase in unbonded post-tensioned members strengthened with EB techniques [4, 5, 12, 13]. The use of NSM-CFRP is commonly accompanied by the concrete cover separation, which limits the reinforcing elements' contribution to increasing flexural capacity and reducing ductility. As a result, the use of U-wrap anchorages, which prevent the concrete cover from separating, is effective in increasing the strains of each of the reinforcing elements, resulting in considerably improved flexural behavior of the reinforced concrete members [10, 14, 15].

Corresponding author: Abbas j. Daraj

The current study is a part of an investigating research regarding the efficiency of strengthening techniques that is performed at Baghdad University (Civil Engineering Lab) [20]. This paper focuses on the strengthening with the use of CFRP near-surface mounted technique.

II. MATERIAL PROPERTIES AND METHODOLOGY

A. *Design of the Tested Girder*

The experimental program includes 7 UPCs simply supported girders with heights (h) of 300mm, widths (b) of 200mm, lengths (L) of 3000mm, and an effective length (L_O) of 2800mm. The concrete cover was 25mm, except for tensile rebars, which use a cover of 35mm. Compressive and tensile strength, and the modulus of elasticity of concrete were obtained according to ASTM C39, ASTM C496-04, and ASTM C469 respectively. The compressive and tensile strengths of the concrete estimated in 10 concrete cylinders (150mm×300mm) were 44.6MPa and 5.1MPa. The concrete had a slump of 118±10mm (Table I). Four girders strengthened with CFRP laminates using the near-surface mounted technique were tested along with a nondamaged reference girder (REF) and two sub-reference girders (PC1R and PC2R) with damaged strand ratios (SDR) of 14.3% and 28.6%. The patterns of strand damage are illustrated in Figure 1. Two types of steel reinforcement with diameters of 16mm and 10mm, as shown in Table II, were used for all girders in tension and compression zones respectively. The appropriate amount of steel was used for shear reinforcement to avoid the occurrence of shear failure before flexural failure. Accordingly, closed stirrups with a diameter of 10mm and a spacing of 100mm c/c were placed along a length of 500mm from the girder's edges and 200mm c/c for the remaining middle length. Two seven-wire low relaxations strands with 12.7mm diameter and Grade 270 were used for each UPC girder (Table II) with a constant eccentricity of 70mm extended inside PVC tubes as unbonded pre-stressing steel. Strand wires were carefully damaged as a result of the spiral form by fastening the two ends of the strand with metal cages and using an electric saw to achieve the specific ratio. Wedge-anchored prestressing strands were directly supported on a steel bearing plate (200mm [width] × 80mm [depth] × 12mm [thickness]) attached to the ends of the girder. Two holes were formed on the steel plate to facilitate the application of prestressing. The steel plate was then installed on the formwork before pouring the concrete to ensure the centrality of strands and achieve complete contact with the concrete.

Four damaged girders were strengthened using the near-surface mounted technique utilizing two CFRP laminates with dimensions of 1.2mm width, 25mm depth, and 2000mm length (Table III)cfrp properties. In addition, two of these girders were strengthened with CFRP U-wrap sheet anchors at the ends of the CFRP laminates with 250mm width and 280mm height (Table IV). The details of the tested girders are presented in Figures 2-4 and Table IVcfrp properties. Girders were post-tensioned by strands (according to the specific damage ratios of each strand) with a straight trajectory after 28 days of casting and immediately before the strengthening process. The initial jacking stress in each strand was $0.6f_{pu}$ (Figure 5). The CFRP laminates were installed one day after the tensioning of girders and before installing the strengthening material, groove locations are first marked on the girders, which have been turned upside down. The concrete was cut to the required dimensions with a concrete saw. An air and water pressure jet was subsequently used to remove the remaining concrete particles in the grooves. CFRP laminates were then inserted after the application of an adhesive layer. The adhesive was leveled with the concrete surface with a scraper (Figure 6). Each strengthened girder contained grooves with dimensions of 30mm (depth) × 6mm (width), as recommended by the ACI 440.2R-17 [11]. The cross-sectional edges of the girders were rounded to a radius of approximately 13mm before applying the carbon panels. Using a grinder, the surface of the specimens was cleaned and prepared for installation. This was done to get rid of laitance and open up the pores in concrete. After that, a primer was used to seal all the possible openings and cracks, and the CFRP sheets were applied using adhesive, according to the manufacturer's instructions (Figure 6).

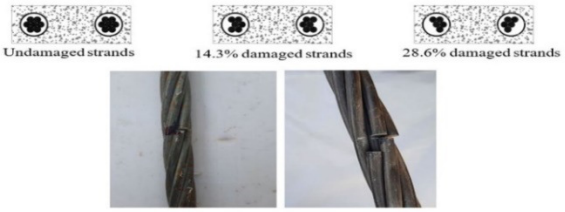

Fig. 1. Patterns of damaged strands in the tested girders.

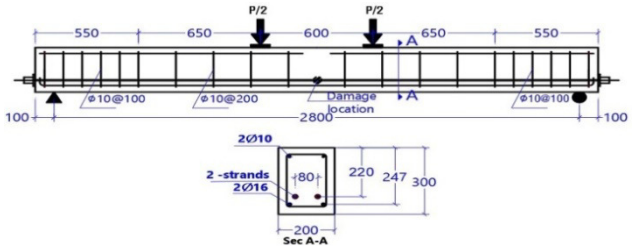

Fig. 2. Details of steel reinforcement and girder profile for the tested girders (all dimensions are in mm).

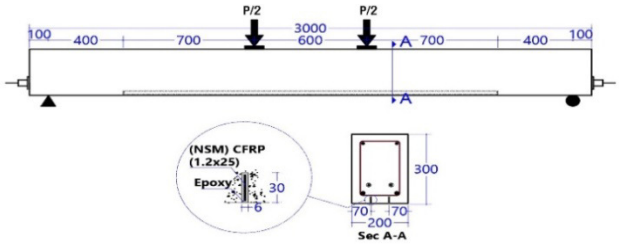

Fig. 3. Details of CFRP-NSM strengthened girders (all dimensions are in mm).

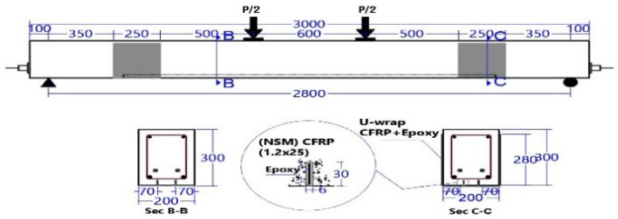

Fig. 4. Details of the CFRP-NSM strengthened girders with U-wrap anchorages (all dimensions are in mm).

Fig. 5. Posttensioning process of the tested girders.

Fig. 6. Strengthening stages of the tested girders.

TABLE I. CONCRETE PROPERTIES

Compressive strength f'_c (MPa)	Tensile strength f_{ct} (MPa)	Modulus of elasticity E_c (MPa)
44.6	5.1	31,220

TABLE II. STEEL REINFORCEMENT PROPERTIES

Type	Dia (mm)	Yield strength (MPa)	Ultimate strength (MPa)	Maximum elongation (%)	Modulus of elasticity (GPa)
rebar	10	518.2	658.97	12.2	200
rebar	16	577.3	710.74	13.4	200
strand	12.7	1725	1860	5	197.5

TABLE III. CFRP PROPERTIES

Material	Thickness (mm)	Tensile modulus (GPa)	Tensile strength (N/mm²)	Ultimate elongation (%)
laminates	1.2	170	3100	2
sheets	0.167	220	3500	1.59

B. Instrumentation and Testing Procedures

The UPC girders were examined under two-point loading, as presented in Figure 7. The load was applied at a distance of 1100mm from the closest support. The strain of the CFRP laminate was detected using strain gauges (with resistance of 119.5±0.5Ω), which were glued to the surface of the CFRP laminate at midlength. The tendon strain was measured using three strain gauges (119.5±0.5Ω) mounted at midlength and loading locations. Notably, grooves were cut in the steel plate before installing anchors to prevent damaging the strain gauge wires. The strain of steel reinforcement was measured using one strain gauge (118.5±0.5Ω) glued at the midlength, whilst two strain gauges (120±0.5Ω resistance and 60mm gauge length) were surface-attached at compression and tension zones to monitor concrete strain. In addition, LVDTs were used to determine the girders' deflection. The data were automatically collected using a computerized data collecting system. To progressively raise the load, a hydraulic jack with 50-ton capacity was used. A load cell with a 50-ton capacity was used to detect the load. The load was applied in increments of 15kN until the cracking load was reached. Then the load was applied in increments of 30kN until failure. Each beam took 2 to 3 hours to complete the test. Two dial gauges were used, one at the end of each strand, to check whether any strand slip occurred during the loading process.

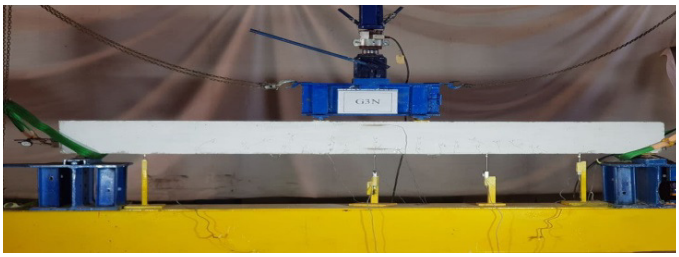

Fig. 7. Test setup of the experimental girders.

TABLE IV. SUMMARY OF THE TEST PARAMETERS

Girder ID	SDR (%)	A_{ps} (mm²)	ρ_p (%)	ρ_s (%)	CFRP laminate $n\times(b_f\times h_f)$ (mm)	U-wrap anchor	
						W_f	H_f
REF	0.0	197.4	0.49	0.81	---	---	---
PC1R	14.3	169.2	0.39		---	---	---
PC1N		169.2			2×1.4×25	---	---
PC1NE		169.2			2×1.4×25	250	280
PC2R	28.6	141.0	0.32		---	---	---
PC2N		141.0			2×1.4×25	---	---
PC2NE		141.0			2×1.4×25	250	280

Note: SDR:Strand Damage Ratio; n, b_f, and h_f : width, and height of CFRP laminates; W_f and H_f : width and height of sheet anchors

III. RESULTS AND DISCUSSION

A. Failure Mode

Flexural failure was observed in reference and sub-reference girders, with tensile steel reinforcing yielding, followed by concrete crushing in the compression zone, as shown in Figures 8(a)-8(c). Compared with the strengthened girders, cracks develop faster, in fewer numbers, and with a wider crack width in the reference and sub-reference girders. The first flexural crack appears in the midspan of sub-reference girders PC1R, and PC2R, with cracking loads of the reference girder's cracking load at approximately 94%, and 85% respectively. It was noticed that the cracking load decreases with increasing Strand Damage Ratio (SDR). The failure modes of the NSM-CFRP-strengthened girders were yielding of the tensile steel reinforcement and concrete cover separation after that (Figures 8(d)-8(f)**Error! Reference source not found.**). The failure of this type of strengthening showed higher brittleness, more cracks, and smaller crack widths than the corresponding sub-reference girders (Figure 9). The first flexural crack appears at the midspan of NSM-CFRP-strengthened girders PC1N, and PC3N, with an increase in the cracking load of 11%, and 13% respectively, compared with those of sub-reference girders. Similar to the reference girders, the strengthened girders with end CFRP U-wrap sheet anchorages failed due to tensile steel reinforcement yield

followed by concrete crushing in the compression zone with more ductility as a result of exploiting the greatest amount of high tensile stress in CFRP laminates before concrete crushing (Figures 8(e), 8(g)). The CFRP U-wrapped anchors, on the other hand, did not affect the tested girder's cracking load. In comparison to the sub-reference girders, flexural cracks arise in the mid-span of the girders PC1NE and PC3NE, with a 13.5% and 13% increase in cracking load. The CFRP U-wrap sheet anchors change the failure mechanism of CFRP NSM laminates significantly. Without CFRP U-wraps, all NSM strengthened girders failed by separating the concrete cover, whereas CFRP U-wraps shift the failure mode to crushing concrete in the compressive zone. A crushing sound indicated the debonding of the CFRP laminate at approximately 85% of the ultimate load. However, the separation of the concrete cover occurred close to the end of CFRP laminates and developed rapidly along the shear span. According to the observations, concrete cover separation was caused by the significant increase of diagonal shear cracks that caused slip along the longitudinal steel reinforcement and the concrete cover. Concrete cover separation or cover delamination and debonding of FRP from the concrete substrate are two failure modes associated with FRP strengthening. They are discussed in detail in [11].

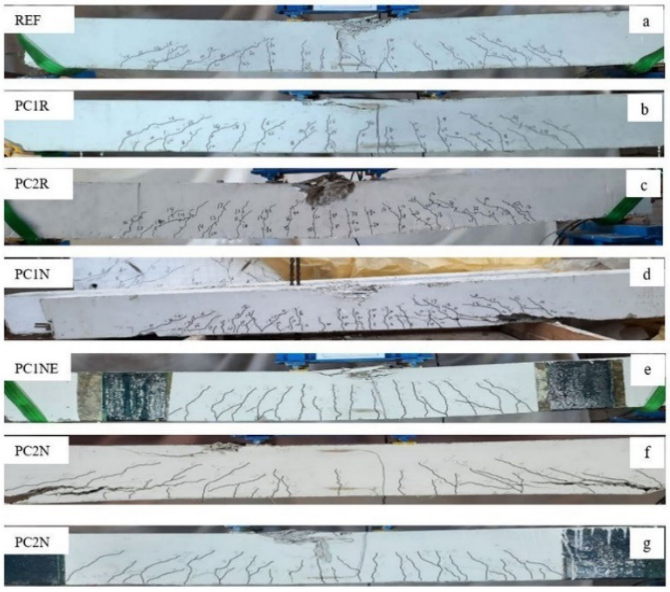

Fig. 8. Failure patterns of the tested girders.

Fig. 9. Concrete cover separation and debonding of CFRP laminates.

B. Load–Deflection Response

The flexural behavior of the studied girders, as shown in Figure 10, was investigated at 3 loading stages: elastic uncracked, allowable load at the serviceability state, and ultimate load. The load-displacement relationship of the studied girders exhibited an elastic linear behavior up to the cracking load. During this stage, as the ratio of damaged strands grows, the stiffness of the reference girders decreases slightly, whereas there was no noticeable change in the stiffness of the strengthened girders compared to their counterparts from the sub-reference girders. However, when the applied load exceeds the crack load, the sub-reference girders exhibit a significantly higher rate of stiffness degradation as a result of the reduction in the pre-stress force, and thus an increase in the rate of crack development, increasing deflection. Meanwhile, the flexural-strengthening CFRP NSM laminates demonstrated their effectiveness in delaying the development of cracks and postponing the degradation of the strengthened girders' stiffness [16, 17]. As a result, for the same level of applied load, the strengthened girders showed lesser deflection than the reference girders.

The applied load of the reference girder was $P_{ser,REF}$= $0.79P_{u,REF}$ when it increased to a load level that caused a deflection corresponding to the permissible deflection (L_o/250=11.2mm) at the serviceability state. This load is denoted by the allowable load at the serviceability state ($P_{ser,REF}$). At the service load ($P_{ser,REF}$), the deflection of sub-reference girders PC1R and PC2R increases by 6.2% and 30.4% respectively, over the reference girder REF. In comparison with their sub-reference counterparts, the deflection of PC1N and PC2N NSM strengthened girders without anchors was reduced by 15.5% and 17.2% respectively, whereas the deflection of PC1NE and PC2NE strengthened girders with anchors was reduced by 14 % and 25% respectively. The flexural strength of the strengthened girders was much higher than that of the reference girder (Table V) and the strength increased with the use of CFRP U-wrap anchorages. During this period, the CFRP U-wrapped anchorage system eliminated the relative slippage and concrete cover delamination of the CFRP laminates and thus significantly enhanced the FRP-strengthening effectiveness and the flexural strength of the girders. In comparison with the reference girder, the flexural capacity of girders PC1R and PC2R was reduced by 5.7% and 11.8% respectively. Compared to their counterparts from the sub-reference girders, the flexural capacity of the strengthened girders without anchors increased by 17.3% and 20.4% respectively, and the flexural capacity of the strengthened girders with anchors increased by 27.9% and 30.1% respectively. It is evident from the results that the effectiveness of the FRP-strengthening increases with the increase in the ratio of damaged strands.

It is essential to compare the behavior of the strengthened girders and the reference girder because it was found that after cracking load, the strengthened girders PC1N and PC1NE (with an SDR of 14.3%) behave similarly to the reference girder until the steel reinforcement yields, resulting in a significant increase in deflection in the reference girder due to the rapidly increasing crack width, while PC1N and PC1NE

maintain a large portion of their stiffness even after yielding of the reinforcing steel until concrete cover separation occurred. Moreover, the deflection of the strengthened girders PC2N and PC2NE (with an SDR of 28.6%) after cracking load is larger than that of the reference girder at the same load level for a load of 85% of the reference girder's ultimate load, which is approximately equal to the yield load of the reinforcing steel. This finding suggests that evaluating the serviceability requirements of prestressed concrete members with more than 14% of damaged strands before implementing repair techniques is crucial despite the restoration of flexural capacity.

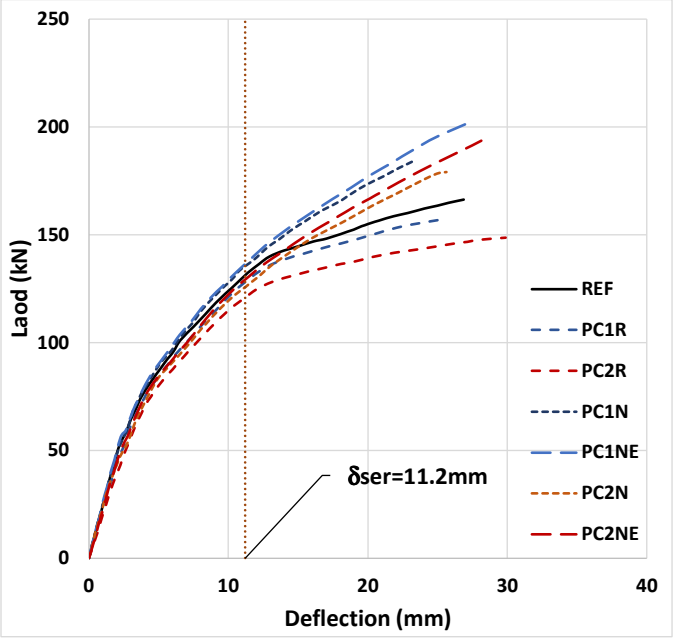

Fig. 10. Load-deflection relationships at mid-span of the tested girders.

TABLE V. SUMMARY OF THE TEST PARAMETERS

Girder ID	P_{cr} (kN)	Pu (kN)	$\delta_{u,mid}$ (mm)	M_u (kN.m)	Reduction in FS relative to RFP (%)	Increase in FS relative to RFP (%)	Failure mode
REF	55	166.24	26.9	91.43	---	---	SY-CC
PC1R	52	157.25	25.5	86.49	5.7	---	SY-CC
PC1N	58	184.56	23.4	101.51	---	11	SY-CCS-CC
PC1NE	59	201.20	26.9	110.66	---	21	SY-CC
PC2R	47	148.72	29.9	81.80	11.8	---	SY-CC
PC2N	53	179.10	25.4	98.51	---	7.7	SY-CCS-CC
PC2NE	53	193.62	28.1	106.49	---	16.5	SY-CC

P_{cr}: f irst cracking load, Pu: ultimate load, δ_u: ultimate deflection, M_u: ultimate load, FS: flexural strength, SY: bonded steel yielding, CC: concrete crushing, and CCS: concrete cover separation

C. Strain in CFRP Laminates

Load versus strain of CFRP laminates is presented in Figure 11. Before the breaking load, the strain in CFRP laminates is minimal and roughly equal, and it is independent of the fastening systems. After the cracking load, the strain rises noticeably and the rate of strain development increases dramatically after the bonded steel reinforcement yields. On the other hand, the strain increases in CFRP laminates with and without anchors were nearly the same, whereas the maximum strain in CFRP laminates with anchors was substantially higher than in those without anchors. The maximum strain of the CFRP laminates in the girders without anchors, PC1N and PC2N, was 0.667% and 0.86% respectively, corresponding to 33.35% and 43% of the rupture strain from coupon tests (ε_{ffu}=2%). On the other hand, the maximum strain of the CFRP laminates in the girders with anchors, PC1NE and PC2NE, was 0.78% and 0.96% respectively, corresponding to 39% and 48% of the rupture strain from the coupon tests. Furthermore, the use of FRP strengthening had a considerable influence on concrete strain. CFRP laminates, as previously stated, successfully reduced cracks and delayed their development. This behavior resulted in a higher compressive concrete zone height for NSM-CFRP-strengthened specimens, resulting in lower concrete strain in the strengthened girders at the same loading level as sub-reference girders.

D. Strain in Strands and Influence of CFRP Laminates

The flexural strength remained unaffected by the strands before the occurrence of the first crack because of the small strain increases. Notably, the strand strain increase was determined by subtracting the initial strain (≈0.46%) from the actual strain, as illustrated in Figure 11. The behavior of strands was very similar amongst the investigated specimens during this stage. The strain of strands began to increase significantly after cracking. The increase in strand strain of sub-reference specimens was higher than that of the reference girder. However, at the same loading level, the increase in strand strain of NSM-CFRP specimens was less than that of the sub-reference specimens. At the reference girder's permissible load ($P_{ser\text{-}REF}$), the increase in the strand strain was about 0.0693% whereas the corresponding increase in strand strains in sub-reference girders, PC1R and PC2R, was 0.0752% and 0.0896% respectively, which showed an increase of 8.6% and 29.5% in comparison with the reference girder REF. Similarly, the strand strain increase in strengthened girders without anchors, PC1N and PC2N, was 0.0651% and 0.0731%, with a reduction of 15% and 22% compared with their counterparts in the sub-reference girders. On the other hand, the strand strain increases in strengthened girders with anchors, PC1NE and PC2NE, was 0.0621%and 0.0712%, with a reduction of 20.7% and 26% compared with their counterparts in the sub-reference girders.

In the loading phase, after the allowable load at the serviceability state, the strand strain increase in the strengthened girders was much smaller than that in the reference girder at the same loading level. For instance, at the maximum load of the reference girder ($P_{u,REF}$), the strand strain increase in the strengthened girders without anchors, PC1N and PC2N, was smaller by 42% and 25.5%. Similarly, the strand strain increase in the strengthened girders with anchors, PC1NE and PC2NE, was smaller by 52.6% and 29%. The CFRP laminates and CFRP U-wrapped anchorages have a considerable influence on the behavior of the strands. Again, the CFRP laminates were able to arrest cracks and delay crack development and they slowed down the degradation of the girder stiffness.

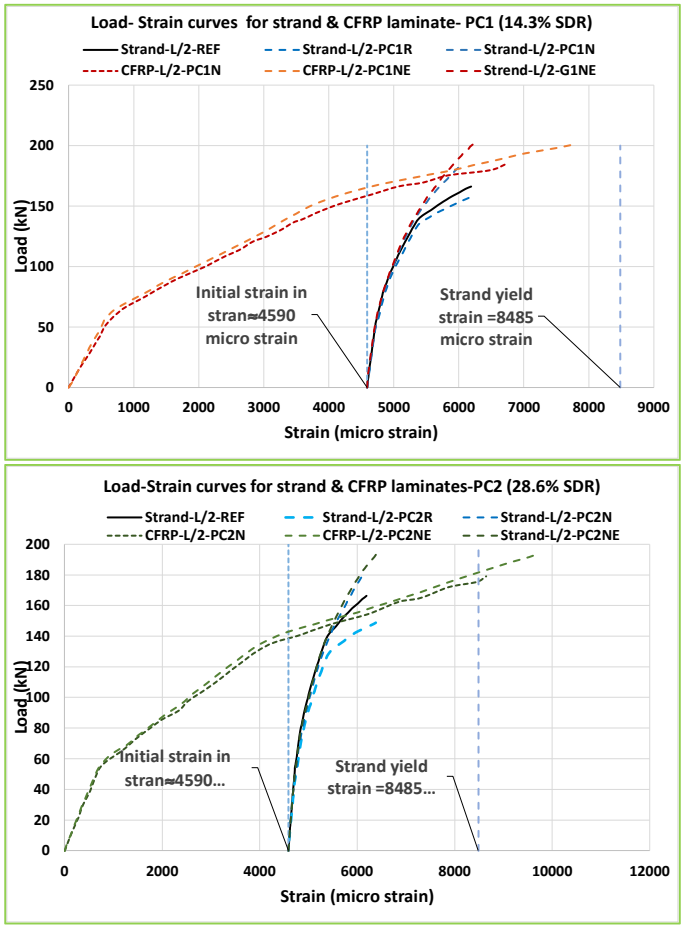

Fig. 11. Load-strain curves of CFRP laminates and strands.

IV. STRAIN INCREASE OF THE STRANDS

Determining the increase in a strain of unbonded strands is a critical case in estimating the flexural strength of unbonded post-tensioned members strengthened with near-surface mounted CFRP laminates. Unfortunately, the design guidelines have only proposed one approach to evaluate the increase in the strain of bonded strands in bonded post-tensioned and pre-tensioned members strengthened with EB-CFRP sheets, whereas the corresponding approaches for unbonded strands in members strengthened with NSM-CFRP laminates are not included. Additionally, the experimental results have exhibited that NSM-CFRP laminates significantly influence the unbonded tendons' behavior. The strand's strain increase of the unbonded post-tensioned members strengthened with CFRPs was evaluated using Tam and Pannell's equations for unbonded tendons in normal reinforced concrete members. For members without end CFRP U-wrapped sheet anchorages, we have:

$$\Delta_{\varepsilon ps,CFRP} = \Omega\varepsilon_c\left(\frac{d_p-c}{L_0}\right)\times\left(1+100\frac{A_f E_f \varepsilon_{fe}}{A_c E_c \varepsilon_{fuu}}\right)^{0.59} \quad (1)$$

For members with CFRP U-wrapped sheet anchorages:

$$\Delta_{\varepsilon ps,CFRP} = \Omega\varepsilon_c\left(\frac{d_p-c}{L_0}\right)\times\left(1+100\frac{A_f E_f \varepsilon_{fe}}{A_c E_c \varepsilon_{fuu}}\right)^{1.35} \quad (2)$$

After that, the overall strain of the unbonded strands $\Delta_{\varepsilon ps,CFRP}$ is calculated as:

$$\varepsilon_{ps,CFRP} = \varepsilon_{pe} + \Delta_{\varepsilon ps,CFRP} \quad (3)$$

where ε_{fe} is the initial strain of strands not including strain losses = $F_p/(E_p A_p)$, F_p (N) is the actual tensile force in strands, A_p (mm^2) and E_p (MPa) are the cross-sectional area and the elasticity modulus of a strand respectively, $\Delta_{\varepsilon ps,CFRP}$ is the increase in the strain of strands, ψ is the length of the plastic zone divided by the height of the compressive concrete zone: Ω = 10.5 [18] for simply supported unbonded post-tensioned members which are un-cracked and reinforced with CFRP laminates, and Ω = 9.8 [4] for the pre-cracked unbonded post-tensioned members reinforced by EB-CFRP sheets. ε_c is the maximum strain at concrete compression fiber as per ACI 440.2R-17 [11], d_p (mm) is the distance between the compressive concrete zone's furthest point and the centroid of the strand cross-sectional area, c (mm) is the compressive concrete zone's height as per [19], L_0 (mm) is the effective span of the members, and ε_{fe} is the actual strain in CFRP laminates at the ultimate applied load.

V. THE PROPOSED FORMULA'S EVALUATION

Equations (1)–(13) were applied to the estimating flexural strength of the 23 unbonded post-tensioned members reinforced with CFRP laminates including the 7 simply supported members reinforced with EB-CFRP laminates investigated in this manuscript and 16 slabs and girders from [4]. The predicted flexural strength, $M_{u,pred}$ was calculated as per ACI 440.2R-17 [11] considering the materials and strength reduction factors to be equal to 1.0, as follows:

Step #1: Estimation of the compressive concrete zone depth (c). The depth of the neutral axis, c (mm), is initially assumed, which could be h/10 as per [11], where h is defined as the concrete cross-section height.

Step #2: Evaluating the strain in CFRP laminates, concrete, and strands. The CFRP laminate strain ε_{fe}, for failure detected by concrete crushing is given by:

$$\varepsilon_{fe} = \varepsilon_{cu}\left(\frac{d_f-c}{c}\right) - \varepsilon_{bi} \le \varepsilon_{fd} \quad (4)$$

where d_f is the effective CFRP laminates depth, ε_{cu} is the concrete's ultimate compressive strain which is equal to 0.003, c is the compressive concrete zone depth, and ε_{bi} is the initial strain in substrate:

$$\varepsilon_{bi} = \frac{-F_p}{E_c A_c}\left(1+\frac{e\, y_b}{r^2}\right)+\frac{M_{DL} y_b}{I_c A_c} \quad (5)$$

where F_p (N) is the initial prestressing force after excluding the losses, e (mm) is the prestressing force's eccentricity concerning the concrete cross-centroid section, y_b (mm) represents the distance from the gross-centroidal section (ignoring steel rebars) to the farthest bottom fiber, r (mm) represents the radius gyration of the member section = $(I_c/A_c)^{0.5}$, I_c (mm^4) represents the moment of inertia of concrete cross concerning the neutral axis, M_{DL} (N.mm) is the applied dead load's moment, and ε_{fd} is the strain's debonding described by:

$$\varepsilon_{fd} = 0.41\sqrt{\frac{f_c'}{nE_c t_f}} \leq 0.9\varepsilon_{ffu} \quad (6)$$

$$\varepsilon_{fd} = 0.7\ \varepsilon_{ffu} \quad (7)$$

where fc' is the concrete strength, ε_{ffu}, t_f, and E_f are the ultimate strain, thickness, and elasticity modulus of CFRP respectively, and n represents the CFRP layers numbers. According to [11], (6) is replaced by (7) to determine the debonding strain of NSM-CFRP in this study.

The strain in CFRP laminates, ε_{fe}, for failure caused by rupture of strands is:

$$\varepsilon_{fe} = \left(\varepsilon_{pu} - \varepsilon_{pi}\right)\left(\frac{d_f - c}{c}\right) - \varepsilon_{bi} \leq \varepsilon_{fd} \quad (8)$$

where ε_{pu} is the strands rupture strain which is equal to 0.05 and ε_{pi} is the strand initial strain, which can be estimated as:

$$\varepsilon_{bi} = \frac{F_p}{E_c\, A_c} + \frac{F_p}{E_c\, A_c}\left(1 + \frac{e^2}{r^2}\right) \quad (9)$$

Step #3: Estimation of the steel rebars strain ε_s:

$$\varepsilon_s = \left(\varepsilon_{fe} + \varepsilon_{bi}\right)\left(\frac{d - c}{d_f - c}\right) \quad \text{for tensile rebars} \quad (10)$$

Step #4: Recalculation of the depth of the compressive concrete zone c using the equilibrium of forces:

$$c = \frac{A_p f_{ps} + A_s f_s + A_f f_{fe}}{\alpha_1 f_c' \beta_1 b} \quad (11)$$

where f_{fe} (MPa) is the CFRP laminates stress = $E_f \times \varepsilon_{fe}$, f_{ps} (MPa) is the strands stress = $E_p \times \varepsilon_{ps,CFRP} \leq f_{py}$, and f_s (MPa) is the tensile rebars stress = $E_s \times \varepsilon_s \leq f_y$.

Step #5: Checking the depth of the compressive concrete zone c. If the assumed value of c (c_{assu}) and re-calculated one (c_{calc}) meet the presented convergence criterion in (12), the appropriate value of c is obtained. If not, the value of c_{assu} is recalculated and the process is repeated starting at the second step until convergence is achieved.

$$\text{Criterion of convergence} = \frac{|c_{assu} - c_{cal}|}{c_{assu}} \leq 0.1\% \quad (12)$$

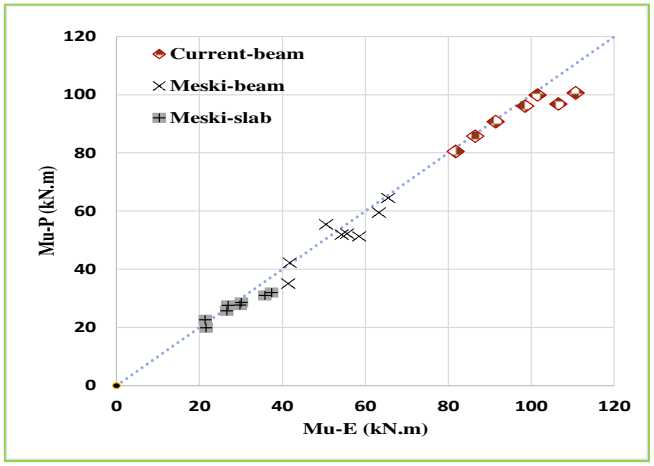

Fig. 12. Experimental vs. predicted values of flexural capacities.

Step #6: Evaluating the flexural strength of NSM-CFRP strengthened members. Finally, the flexural strength of NSM-CFRP strengthened unbonded post-tensioned members, $M_{u\text{-}P}$, can be calculated as per (13):

$$M_{u-P} = A_p f_{ps}\left(d_p - \frac{\beta_1 c}{2}\right) + A_f f_{fe}\left(d_f - \frac{\beta_1 c}{2}\right) + A_s f_s\left(d - \frac{\beta_1 c}{2}\right) \quad (13)$$

The predicted-to-experimental flexural strength ratios $M_{u\text{-}P}$ /$M_{u\text{-}E}$ are illustrated in Table VI and **Error! Reference source not found.**Figure 12. The mean value is 0.948 and COV=0.066 (Coefficient Of Variation). They describe the accuracy of the theoretical strand strain values and their suitability for the prediction of the flexural strength of the NSM-CFRP unbonded post-tensioned members with and without anchorages.

TABLE VI. TABLE I: THE PREDICTED AND EXPERIMENTAL FLEXURAL CAPACITIES

EB CFRP-strengthened UPC members El Meski and Harajli			
Specimens	$M_{u\text{-}P}$	$M_{u\text{-}E}$	$M_{u\text{-}P}$ / $M_{u\text{-}E}$
Girders			
UB1_H_F1	41.36	41.80	0.99
UB1_H_F2	51.38	54.30	0.95
UB1_P_F1	34.75	41.40	0.84
UB1_P_F2	51.68	55.60	0.93
UB2_H_F1	54.85	50.50	1.09
UB2_H_F2	63.86	65.50	0.97
UB2_P_F1	50.79	58.50	0.87
UB2_P_F2	58.91	63.30	0.93
Slabs			
US1_H_F1	22.37	21.40	1.05
US1_H_F2	27.32	26.90	1.02
US1_P_F1	19.70	21.60	0.91
US1_P_F2	28.31	30.10	0.94
US2_H_F1	25.44	26.60	0.96
US2_H_F2	30.69	35.80	0.86
US2_P_F1	27.42	29.80	0.92
US2_P_F2	31.68	37.40	0.85
Average			0.941
Standard of deviation			0.070
COV			0.075
NSM-CFRP strengthened UPC girders (current study)			
REF	90.72	91.43	0.992
PC1R	85.72	86.49	0.991
PC1N	99.88	101.51	0.984
PC1NE	100.65	110.66	0.909
PC2R	80.50	81.80	0.984
PC2N	96.05	98.51	0.975
PC2NE	96.79	106.49	0.909
Average			0.964
Standard of deviation			0.038
COV			0.039
For all members			
Average			0.948
Standard of deviation			0.062
COV			0.066

$M_{u\text{-}P}$ is the predicated moment capacity and $M_{u\text{-}E}$ is the experimental moment capacity

VI. CONCLUSIONS

The behavior of post-tensioned concrete girders subjected to partial strand damage and strengthened by NSM-CFRP laminates with and without CFRP U-wrap sheet anchorages

was researched and evaluated in this work. The following conclusions are derived from this study's experimental results:

- The flexural capacity of post-tensioned girders reduces as the SDR increases. The flexural strength was reduced by 6% and 12% for girders with strand damage of 14.3% and 28.6% respectively. On the other hand, at all loading stages, the deflection increases as the SDR increases.
- Near-surface mounted techniques using CFRP laminates enhance flexural capacity by controlling crack development. In comparison with the nondamaged girder, the NSM-CFRP laminates enhanced the flexural capacity by 11% corresponding to strand damage of 14.3%, whereas the flexural capacity increased by 7.7%, corresponding to strand damage of 28.6%.
- The use of U-wrap anchorages eliminates the cover separation and effectively enhances the flexural strength for strengthened girders. In comparison with the nondamaged girder, the NSM-CFRP laminates enhanced the flexural capacity by 21% corresponding to strand damage of 14.3%. whereas the flexural capacity increased by 16.5%, corresponding to strand damage of 28.6%.
- The CFRP laminates significantly affect the behavior of the strands. At the same loading level, the strain increase of the strands in the strengthened girders was much smaller than that of the damaged girder. For example, at the service load of the undamaged reference girder, the increase in strand strain of the strengthened girders is reduced by 15% and 22% respectively, compared to the increase in strand strain of the corresponding damaged girders. On the other hand, this effect increases considerably when using U-wrap anchorages.
- The proposed procedure for predicting strand strain rises in unbonded post-tension girders enhanced with NSM-CFRP laminates, effectively predicts flexural strength with high accuracy and minimal variation (average = 0.956 and COV = 0.064).

REFERENCES

[1] C. E. Reed and R. J. Peterman, "Evaluation of Prestressed Concrete Girders Strengthened with Carbon Fiber Reinforced Polymer Sheets," *Journal of Bridge Engineering*, vol. 9, no. 2, pp. 185–192, Mar. 2004, https://doi.org/10.1061/(ASCE)1084-0702(2004)9:2(185).

[2] O. Rosenboom, T. K. Hassan, and S. Rizkalla, "Flexural behavior of aged prestressed concrete girders strengthened with various FRP systems," *Construction and Building Materials*, vol. 21, no. 4, pp. 764–776, Apr. 2007, https://doi.org/10.1016/j.conbuildmat.2006.06.007.

[3] M. Di Ludovico, A. Prota, G. Manfredi, and E. Cosenza, "FRP Strengthening of Full-Scale PC Girders," *Journal of Composites for Construction*, vol. 14, no. 5, pp. 510–520, Oct. 2010, https://doi.org/10.1061/(ASCE)CC.1943-5614.0000112.

[4] F. El Meski and M. Harajli, "Flexural Behavior of Unbonded Posttensioned Concrete Members Strengthened Using External FRP Composites," *Journal of Composites for Construction*, vol. 17, no. 2, pp. 197–207, Apr. 2013, https://doi.org/10.1061/(ASCE)CC.1943-5614.0000330.

[5] L. Nguyen-Minh *et al.*, "Flexural-strengthening efficiency of cfrp sheets for unbonded post-tensioned concrete T-beams," *Engineering Structures*, vol. 166, pp. 1–15, Jul. 2018, https://doi.org/10.1016/j.engstruct.2018.03.065.

[6] B. F. Abdulkareem, A. F. Izzet, and N. Oukaili, "Post-Fire Behavior of Non-Prismatic Beams with Multiple Rectangular Openings Monotonically Loaded," *Engineering, Technology & Applied Science Research*, vol. 11, no. 6, pp. 7763–7769, Dec. 2021, https://doi.org/10.48084/etasr.4488.

[7] H. M. Hekmet and A. F. Izzet, "Performance of Segmental Post-Tensioned Concrete Beams Exposed to High Fire Temperature," *Engineering, Technology & Applied Science Research*, vol. 9, no. 4, pp. 4440–4447, Aug. 2019, https://doi.org/10.48084/etasr.2864.

[8] S. Erdemlı Gunaslan, A. Karasin, and M. Öncü, "Properties of FRP Materials for Strengthening," *International Journal of Innovative Science, Engineering & Technology*, vol. 1, no. 9, pp. 656–660, Dec. 2014.

[9] A. Soror, M. Tayel, and K. Heiza, "Post-tensioned Reinforced Concrete Beams Strengthend With Near Surface Mounted Technique," Dec. 2018, https://doi.org/10.13140/RG.2.2.31671.78247.

[10] A. Hosen, Z. Jumaat, K. M. ud Darain, and M. Obaydullah, "Innovative End Anchorage for Preventing Concrete Cover Separation of NSM Steel and CFRP bars Strengthened RC Beams," presented at the 6th Jordanian International Civil Engineering Conference, Amman, Jordan, Mar. 2015.

[11] ACI-Committee-440.2R-17, *ACI PRC-440.2-17: Guide for the Design and Construction of Externally Bonded FRP Systems for Strengthening Concrete Structures*. West Conshohocken, PA, USA: ACI, 2017.

[12] A. M. Al-Hilali, A. F. Izzet, and N. Oukaili, "Static Shear Strength of a Non-Prismatic Beam with Transverse Openings," *Engineering, Technology & Applied Science Research*, vol. 12, no. 2, pp. 8349–8353, Apr. 2022, https://doi.org/10.48084/etasr.4789.

[13] A. H. Al-Zuhairi and A. I. Taj, "Effectiveness of Meso-Scale Approach in Modeling of Plain Concrete Beam," *Journal of Engineering*, vol. 24, no. 8, pp. 71–80, Jul. 2018, https://doi.org/10.31026/j.eng.2018.08.06.

[14] A. Hasnat, M. M. Islam, and A. F. M. S. Amin, "Enhancing the Debonding Strain Limit for CFRP-Strengthened RC Beams Using U-Clamps: Identification of Design Parameters," *Journal of Composites for Construction*, vol. 20, no. 1, Feb. 2016, Art. no. 04015039, https://doi.org/10.1061/(ASCE)CC.1943-5614.0000599.

[15] I. S. Shabana, I. A. Sharaky, A. Khalil, H. S. Hadad, and E. M. Arafa, "Flexural response analysis of passive and active near-surface-mounted joints: experimental and finite element analysis," *Materials and Structures*, vol. 51, no. 4, Jul. 2018, Art. no. 107, https://doi.org/10.1617/s11527-018-1232-x.

[16] A. H. Al-Zuhairi, A. H. Al-Ahmed, A. A. Abdulhameed, and A. N. Hanoon, "Calibration of a New Concrete Damage Plasticity Theoretical Model Based on Experimental Parameters," *Civil Engineering Journal*, vol. 8, no. 2, pp. 225–237, Feb. 2022, https://doi.org/10.28991/CEJ-2022-08-02-03.

[17] A. A. Abdulhameed *et al.*, "The Behavior of Hybrid Fiber-Reinforced Concrete Elements: A New Stress-Strain Model Using an Evolutionary Approach," *Applied Sciences*, vol. 12, no. 4, Jan. 2022, Art. no. 2245, https://doi.org/10.3390/app12042245.

[18] A. Tam and F. N. Pannell, "The ultimate moment of resistance of unbonded partially prestressed reinforced concrete beams," *Magazine of Concrete Research*, vol. 28, no. 97, pp. 203–208, Dec. 1976, https://doi.org/10.1680/macr.1976.28.97.203.

[19] ACI Committee 318, *ACI CODE-318-19: Building Code Requirements for Structural Concrete and Commentary*. West Conshohocken, PA, USA: ACI, 2019.

[20] H. Q. Abbas and A. H. Al-Zuhairi, "Flexural Strengthening of Prestressed Girders with Partially Damaged Strands Using Enhancement of Carbon Fiber Laminates by End Sheet Anchorages," *Engineering, Technology & Applied Science Research*, vol. 12, no. 4, pp. 8884–8890, Aug. 2022, https://doi.org/10.48084/etasr.5007.